Agricultural and Forest Meteorology 339 (2023) 109582

Contents lists available at ScienceDirect

Agricultural and Forest Meteorology

journal homepage: www.elsevier.com/locate/agrformet

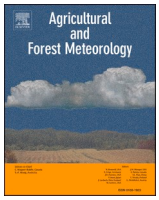

Plant canopies exhibit stronger thermoregulation capability at the seasonal than diurnal timescales

Zhengfei Guo [a], Kun Zhang [a,b], Hua Lin [c], Bartosz M. Majcher [a], Calvin K.F. Lee [a], Christopher J. Still [d], Jin Wu [a,e,*]

[a] Research Area of Ecology and Biodiversity, School for Biological Sciences, The University of Hong Kong, Hong Kong, China
[b] Department of Mathematics, The University of Hong Kong, Hong Kong, China
[c] CAS Key Laboratory of Tropical Forest Ecology, Xishuangbanna Tropical Botanical Garden, Chinese Academy of Sciences, Xishuangbanna, 666303, China
[d] Forest Ecosystems and Society, Oregon State University, Corvallis, OR, 97331, USA
[e] Institute for Climate and Carbon Neutrality, The University of Hong Kong, Hong Kong, China

ARTICLE INFO

Keywords:
canopy temperature
FLUXNET
carbon cycle
transpiration
energy balance
climate change

ABSTRACT

Plant canopy temperature (T_c) plays a crucial role in regulating plant growth and metabolism. Although dominant controls on T_c are observed to differ across timescales, whether this would cause differences in plant thermoregulation capability (PTC) remains unclear, raising concerns about extrapolating findings on plant thermoregulation from one timescale to another. Here we constructed diurnal and seasonal datasets of T_c, air temperature (T_a), and other biotic and abiotic factors from global hourly flux data, and explored diurnal and seasonal variations in PTC (indicated by T_c *vs.* T_a regression slope, with lower slopes indicating higher T_c stability and stronger thermoregulation). Our result revealed significantly lower T_c *vs.* T_a slopes (i.e. stronger PTC) at seasonal than diurnal timescales, primarily due to different transpiration cooling at high T_a between the two timescales. At the diurnal timescale, transpiration rates initially increase before decreasing with T_a after reaching a specific temperature threshold (~85th percentile of T_a; related to midday depression of stomatal activities); Conversely, at the seasonal timescale, transpiration rates consistently increase with T_a (related to the coincidence among high water availability and the peak annual T_a). PTC also displays considerable spatial variability, with latent heat *vs.* net radiation relationship and water availability being the dominant regulators. Collectively, we recommend caution when extrapolating thermoregulation-relevant conclusions drawn from short-term observations to longer-term predictions, and *vice versa*, since they have different patterns and underlying mechanisms.

1. Introduction

Canopy temperature (T_c) importantly mediates plant metabolic rates. Low T_c inhibits the photosynthetic carboxylation rate of plants, while extremely-high T_c can lead to a high catabolic rate (e.g., dark respiration) and even irreversible tissue damage (Jones, 2013; Wright et al., 2017; Still et al., 2021). As a result, the net photosynthesis rate often peaks at an intermediate T_c (Huang et al., 2019). Additionally, T_c also regulates plant transpiration through the interactions between leaf-to-air vapor pressure deficit (VPD) and stomatal behaviors, and in turn is also regulated by this transpiration cooling (Medlyn et al., 2011; Guo et al., 2022). Ultimately, the influence of T_c on plant metabolic rates could affect the health and growth of plant individuals as well as the large-scale water and carbon cycles (Lin et al., 2020; Farella et al., 2022). Therefore, understanding whether and to what extent plants can thermoregulate their T_c to adapt to their living environments for photosynthesis and growth is a central question in ecology, with critical insights for accurate projections of ecosystems' response and resilience to climate change (Pau et al., 2018; Still et al., 2019).

Plant thermoregulation refers to the ability of plants to regulate their T_c within a relatively stable range, despite the variability in T_a (Michaletz et al., 2016; Still et al., 2019; Guo et al., 2023). This ability is influenced by plant functional traits (e.g., intrinsic plant water use strategy, leaf morphology, and canopy structure; Still et al., 2019) and their living environments (e.g. light, VPD, and wind speed; Michaletz et al., 2015) (Fig. 1a). Specifically, plants can be heated up by absorbing solar radiation, while they can also be cooled down through various processes (Campbell and Norman, 2012; Jones, 2013). One common

* Corresponding author at: School for Biological Sciences, The University of Hong Kong, Pokfulam Road, Hong Kong.
E-mail address: jinwu@hku.hk (J. Wu).

https://doi.org/10.1016/j.agrformet.2023.109582
Received 9 May 2023; Received in revised form 18 June 2023; Accepted 25 June 2023

process is transpiration, where plants lose water vapor from their leaves, leading to a cooling effect on T_c. In addition to transpiration cooling, non-evapotranspiration cooling, such as enhancing leaf-to-air heat dissipation, can effectively cool T_c, especially under water-limited conditions (Gates et al., 1968; Rotenberg & Yakir., 2010; Leigh et al., 2017; Muller et al. 2021). Leaf orientation or structure is another method of plant thermoregulation. For example, some plants have leaves that can change orientation to avoid direct sunlight and reduce heat absorption (Ehleringer & Forseth, 1989), and other plants have succulent leaves or hairy surfaces that reduce heat absorption or increase heat dissipation (Wuenscher, 1970).

The issue of whether and to what extent plant thermoregulation occurs remains a topic of debate in biological research (Helliker and Richter, 2008; Drake et al., 2020; Still et al., 2022). Some argue that T_c and air temperature (T_a) are rapidly in equilibrium and can simply be considered equivalent (Drake et al., 2020), while others suggest that T_c is homeothermic despite variations in T_a (Helliker and Richter, 2008). In this study, we used the terminology 'thermoregulation' to describe the systematic deviation of T_c from T_a without implying any specific directionality. To quantify the degree of plant thermoregulation, we used the regression slope between T_c *vs.* T_a as an indicator, as it is a general and widely accepted method (Blonder & Michaletz, 2018; Guo et al., 2023). It is hypothesized that if plant thermoregulation occurred, T_c would change more slowly than T_a over time, leading the T_c *vs.* T_a regression slope to be less than 1. A lower regression slope means higher stability of T_c when facing the dynamics in T_a over time, thus indicating a stronger plant thermoregulation capability (PTC) (Fig. S1; Michaletz et al., 2016; Drake et al., 2020). To date, many empirical studies have shown that the slope metric varies widely across species and biomes (Dong et al., 2017; Blonder & Michaletz et al., 2018; Blonder et al., 2020). For example, across global extratropical vegetated ecosystems, plant ecosystems were observed to exhibit diverse PTC from slope<1 (limited homeothermy) to slope>1.2 (megathermy) (Guo et al., 2023).

Compared with the studies exploring the spatial dynamics mentioned above, understanding the patterns and drivers of diverse plant thermoregulation behaviors across timescales is also important but remains poorly studied. T_c is regulated by both abiotic and biotic factors, with dominant controls varying by timescale (Fig. 1). Within a day, stomatal conductance (Matthews et al., 2018) and leaf angle (for certain species; Ehleringer & Forseth, 1989) can significantly affect T_c by altering the flux of transpiration and/or net radiation (Leuzinger and Körner, 2007). Contrastingly, across seasons, factors such as leaf age demography, canopy structure, and soil water content also play key roles (Still et al., 2021; Jin et al., 2022) (Fig. 1b). Adjust their T_c with seasonal changes has important physiological meaning for plants. Specifically, during early growing seasons with cool temperature, plants may adjust their leaf pigments or angles to increase light absorption that can further increase T_c and thus enhance photosynthetic carbon uptake (Jones, 2013). While during the peak growing seasons with hot temperature, plants usually increase total leaf area and/or change leaf clustering to enhance the transpiration and/or heat dissipation rates, which ultimately help to reduce their T_c (Guo et al., 2023; Muller et al., 2023). These collectively imply that the seasonal thermoregulation could be a strategy to allow plants to adjust their T_c to better adapt to their seasonal climate (i.e., avoiding the heat stress while mitigating the cold temperature impact), thus prompting plant growth. Even though the dominant drivers responsible for T_c vary with the timescale of interest, it has not been assessed whether they would result in distinct PTC across timescales. If such differences were to exist, they would have important implications for applying conclusions drawn from short-term (e.g., diurnal) observations to longer-term (e.g., across seasons) predictions and *vice versa*; thus, they ought to be urgently explored.

To gain an improved understanding of plants' thermoregulation capabilities across diurnal and seasonal timescales, we leveraged global datasets of T_c, T_a, and other environmental and biotic variables from FLUXNET2015, Asiaflux, European flux, and Brazil flux network (see section 2.1 for more details), and comprehensively evaluated the T_c *vs.* T_a relationship at both timescales of interest. We hypothesized that plants exhibit stronger PTC (corresponding to a smaller slope indicator; Fig. S1) across seasonal timescales since more factors and processes are involved in the T_c regulation at this timescale than the diurnal timescale. Accordingly, we asked the following three questions: 1) Do plant canopies show different PTC across diurnal and seasonal timescales? 2) If yes, what are the mechanisms underlying this difference? 3) What are the drivers of spatial variability in PTC across the two timescales of interest? To address these questions, we first explored the thermoregulation patterns and mechanisms of plant ecosystems across diurnal and seasonal timescales, and then used an integrated framework of state-of-the-art machine learning model and game-theory interpretation (i.e., XGB-SHAP; Wang et al., 2022) to assess the relative contribution of each

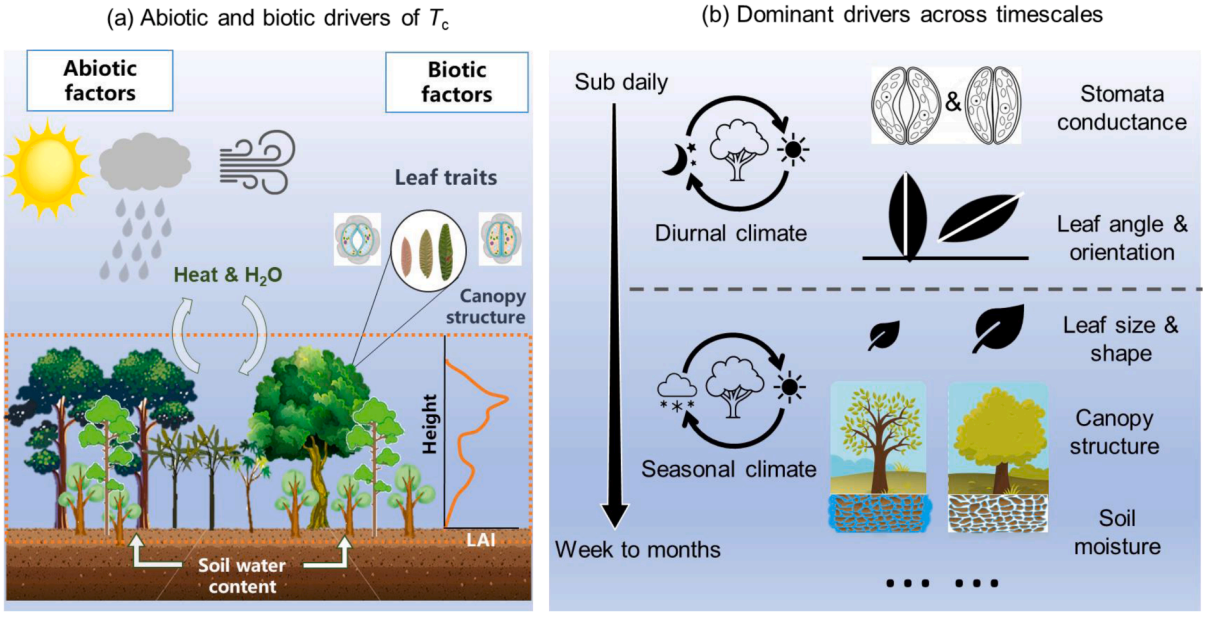

Fig. 1. Abiotic and biotic variables jointly regulate the canopy temperature (T_c) but the dominant factors differ on different timescales. (a) The main factors that regulate T_c include environmental and biological variables. (b) The dominant controls on T_c differ on diurnal and seasonal timescales.

abiotic and biotic variable to the spatial variability in PTC across global flux sites.

2. Materials and methods

2.1. Flux data

We used eddy covariance (EC)-based flux data from FLUXNET2015 (Pastorello et al., 2020), Asiaflux (https://db.cger.nies.go.jp/asiafluxdb/), European flux (https://www.icos-cp.eu/data-products/2G60-ZHAK), and the Brazil flux network (Restrepo-Coupe et al., 2013) (Fig. 2). It includes observations of carbon (e.g., gross primary productivity—GPP), and energy fluxes (e.g., net radiation—R_n, longwave radiation—R_{LW}, sensible heat—H, and latent heat—LE), as well as key meteorological data (e.g., T_a, relative humidity—RH, and windspeed—u, shear velocity—u^*). A total of 155 sites (including 869 site-years observations; Fig. 2), spanning a large latitudinal gradient from 70° N to 37° S were used after removing sites that did not meet our requirements (see Section 2.3.1). This dataset was selected for several reasons. First, the dataset is publicly available and covers major plant functional types (PFTs) around the world. Second, this dataset was processed following a rigorous data-processing pipeline including quality control, gap-filling, and photosynthesis partitioning (Pastorello et al., 2020; Restrepo-Coupe et al., 2013), and provided quality-controlled meteorological and flux data for consistent assessments of T_c *vs.* T_a relationships. Notably, only the measured or gap-filled data with good quality (QC=0 for direct measurements or 1 for good quality gap-filled data) were used in this study, and the energy fluxes data were corrected with the energy balance closure. Third, many models and theories have been developed to infer T_c from these flux measurements with demonstrated accuracy (Doughty & Goulden, 2008; Jones., 2013; Guillevic et al., 2018). Finally, it provides hourly observations and covers the full annual cycle(s), allowing us to extract diurnal and seasonal signals from original flux observations (see Section 2.3.2 for details).

2.2. Satellite and reanalysis-based data

In addition to flux observations, some other abiotic and biotic variables from satellite and reanalysis data were also used as candidate variables for explaining the spatial variability in PTC (indicated by the T_c *vs.* T_a regression slope; Michaletz., et al., 2016; Drake et al., 2020). Specifically, 5 additional abiotic and biotic variables showing direct linkages with the canopy energy balance process were extracted and used, namely, elevation (from SRTM90_V4; Van, 2001), soil water content (SWC, from ERA5L, Muñoz-Sabater et al., 2021), leaf area index (LAI; from MCD15A3H; Myneni & Park, 2015), canopy height (H_c, from ETH_GlobalCanopyHeight_2020_10m_v1, Lang et al., 2022), and plant functional type (PFT; from MCD12Q1, Friedl & Sulla-Menashe, 2015) (Table 1). For each site, the average value of each variable within a 3*3 pixels window around the site was calculated. These datasets were selected for two reasons. First, they are publicly available on Google Earth Engine and have been pre-processed following standard protocols (Gorelick et al., 2017). Second, they have been demonstrated to have high accuracy and are widely used in many global scale studies (Van, 2001; Myneni & Park, 2015; Muñoz-Sabater et al., 2021).

2.3. Methods

A flowchart outlining the full data analysis procedure is provided in Fig. 3, which includes three parts: 1) data processing; 2) evaluating the patterns of PTC at the diurnal and seasonal timescale, respectively; 3) exploring the drivers of spatial PTC variability.

2.3.1. Data processing

1) **Extraction of growing season data for densely vegetated sites.** The flux-derived ecosystem temperature usually includes the temperature of bare soil and plant canopies (Still et al., 2022). To minimize the contamination from the bare soil background (which has a considerable effect in either the early/late growing season with less leaf cover or sparse vegetation with higher soil fraction all year round), we here followed Guo et al. (2023), and only focused on the data within the growing season of densely vegetated sites, in which we assume that plant canopies dominate the ecosystem-scale surface temperature. The detailed implementation includes two steps. Step 1—Identify the growing season. The start and end of the growing season in each year were calculated based on the seasonality of gross primary productivity (GPP) for each site following Piao et al. (2007), including three sub-steps. First, we smoothed the daily EC-derived GPP data with a 10-day moving window and then extracted the maximum (GPP_{max}) and minimum (GPP_{min}) GPP values for each year. Second, we defined 30% of the GPP amplitude (i.e., GPP_{min} + 0.3*(GPP_{max} - GPP_{min}) as the threshold of the growing season, and the period with GPP less than this threshold was labeled as a non-growing season. Finally, we filtered out all the non-growing season observations. Step 2—Identify the densely vegetated sites. The LAI data from MCD15A3H (Myneni & Park, 2015) was used to filter out the sites with sparse vegetation. Following the protocol of Guo et al. (2023), the sites with mean growing season LAI (LAI_{gs}) <

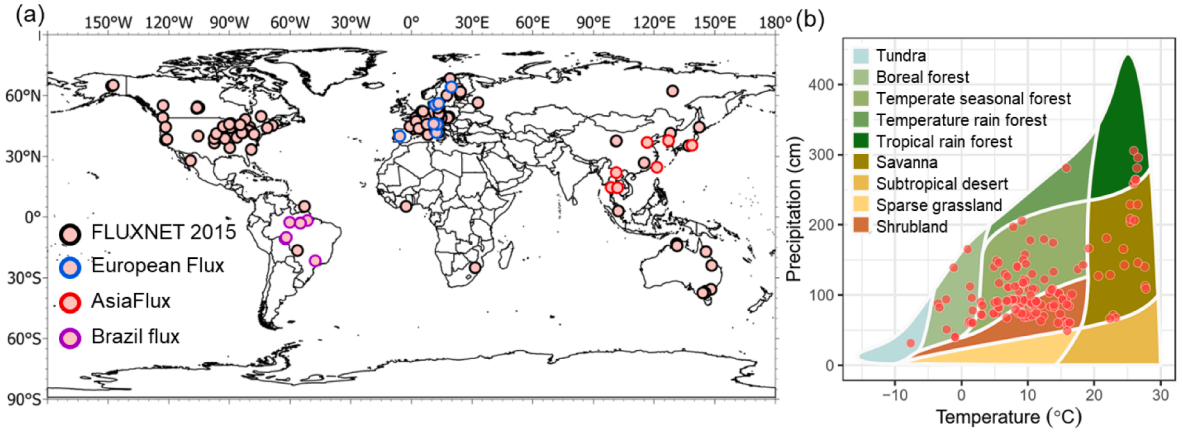

Fig. 2. Distribution of 155 flux sites from FLUXNET 2015, European Flux, AsiaFlux, and Brazil flux (including 869 site-years of observation) used in this study, indicated by circles. (a) Location of each site on latitude and longitude grid; (b) Location of each site on classic Whittaker Biome Classification by the climate of mean annual temperature and precipitation.

Table 1
Summary of the eddy covariance data, remote sensing data, and reanalysis data used in this study.

Variables	Definition	Unit	Resolutions (spatial/temporal)	Data source	Accessed links
T_{c_aero}	Aerodynamic canopy temperature	°C	site/hourly	FLUXNET	A
T_{c_LW}	Radiative canopy temperature	°C	site/hourly	FLUXNET	A
T_a	Air temperature	°C	site/hourly	FLUXNET	A
RH	relative humidity	%	site/hourly	FLUXNET	A
u	Wind speed	m s^{-1}	site/hourly	FLUXNET	A
P	Precipitation	mm	site/hourly	FLUXNET	A
PAR	Photosynthetically active radiation	μmol m^{-2} s^{-1}	site/hourly	FLUXNET	A
GPP	Gross primary productivity	μmol m^{-2} s^{-1}	site/hourly	FLUXNET	A
R_n	Net radiation	W/m^2	site/hourly	FLUXNET	A
LE	Latent heat (evapotranspiration)	W/m^2	site/hourly	FLUXNET	A
H	Sensible heat (convection)	W/m^2	site/hourly	FLUXNET	A
LAI	Leaf area index	m^2/m^2	500m/4day	MCD15A3H	B
Hc	Canopy height	m	30m/-	ETH	C
SWC	Soil water content	% of volume	9km/hourly	ERA5L	D
ε	Canopy surface emissivity	–	500m/daily	MOD21A2	E

A: https://fluxnet.org/data/fluxnet2015-dataset/subset-data-product/.
B: https://lpdaac.usgs.gov/products/mcd15a3hv006/.
C: https://samapriya.github.io/awesome-gee-community-datasets/projects/canopy/.
D: https://www.ecmwf.int/en/era5-land.
E: https://lpdaac.usgs.gov/products/mod21a2v006/.

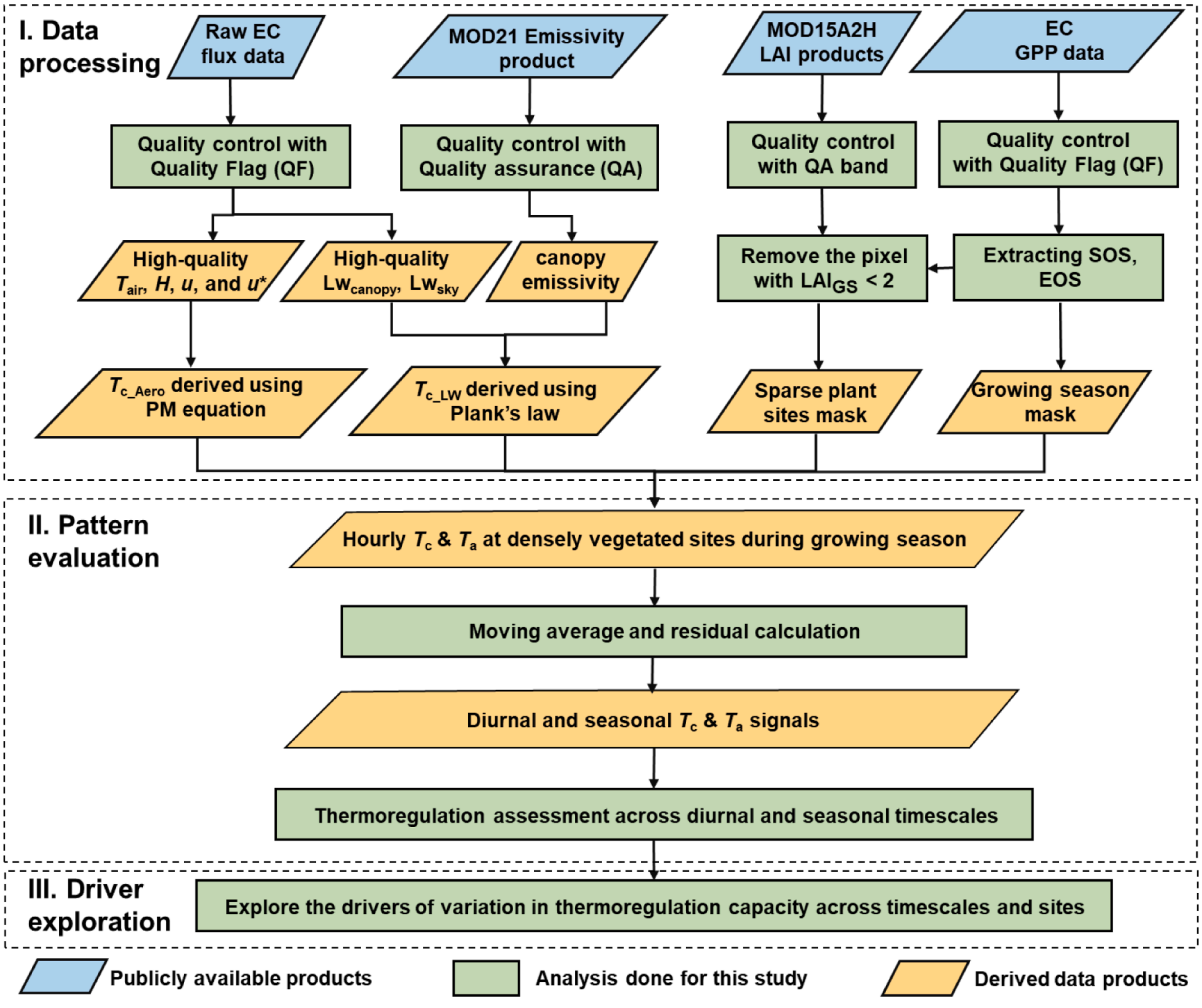

Fig. 3. Workflow for studying the diurnal and seasonal variability in plant thermoregulation capability and its drivers on a global scale.

2.0 m^2/m^2, as well as the observations during the early or late growing season with LAI < 2.0 m^2/m^2, were removed.

2) **Derivation of canopy temperature (T_c).** To derive T_c from the EC flux measurements, two approaches are widely used, including aerodynamic-based (obtaining aerodynamic T_c, i.e., T_{c_Aero}; Eqn. 1) and longwave radiative-based (obtaining longwave-based T_c, i.e., T_{c_LW}; Eqn. 2) (Campbell and Norman, 2012; Jones, 2013). We selected T_{c_LW} as the primary approach because it is independent of

T_a and therefore avoids the recycle use and bias issues when calculating the relationship between T_c and T_a. Meanwhile, when cross-comparing T_{c_LW} with T_{c_Aero}, we found the two T_c metrics and associated T_c *vs.* T_a relationship display very strong agreements with each other (Fig. S2). These T_c metrics were calculated using Eqns. 1 and 2 as follows:

$$T_{c\_Aero} = \left(\frac{u}{(u^*)} + 6.2u^{*-2/3}\right) \times \left(\frac{H}{c_p\rho_a}\right) + T_a \quad (1)$$

$$T_{c\_LW} = \left[\frac{1}{\varepsilon\sigma}\left(LW_{canopy} - (1-\varepsilon)LW_{sky}\right)\right]^{1/4} \quad (2)$$

In Eqn. 1, u is the horizontal wind speed (m/s) obtained from flux data, u^* is the friction velocity (m/s) obtained from flux data, H is the sensible heat flux (W/m^2) obtained from flux data, c_p is the specific heat capacity of air (29.3 J/mol/K), ρ_a is the density of moist air (kg/m3); In Eqn. 2, ε is the emissivity (unitless) obtained from the MODIS emissivity product (MOD21A2), which is averaged within a 3*3 pixel window around the flux site (Guo et al., 2023); σ is the Stefan-Boltzmann constant (5.67 $\times$ 10^{-8} W/m^2/K^4), LW_{canopy} is the upward longwave radiation emitted by the canopy surface (W/m^2) obtained from flux data, and LW_{sky} is the downward longwave radiation emitted by the sky (W/m^2) obtained from flux data.

3) **Remove the *LE* observation on rainy days.** Flux-based *LE* observations are composed of plant transpiration, canopy intercepted evaporation, and soil evaporation (Zhang et al., 2019, 2022). To minimize the interference from the soil evaporation and canopy interception evaporation, we removed *LE* observations on rainy days (daily rainfall > 1mm) and their subsequent 2 days, following Knauer et al. (2018).

2.3.2. *Deriving the patterns of plant thermoregulation capability across timescales*

To answer question 1 (do plant canopies show different thermoregulation capacities across diurnal and seasonal timescales?), we derived PTC (indicated by the regression slope of T_c *vs.* T_a; Fig. S1) at the diurnal and seasonal timescales, respectively. The derivation includes two steps. Step 1—extracting diurnal and seasonal signals, respectively, from hourly EC observations covering the full growing seasons (Fig. 4). For this purpose, we followed Tiwari et al (2013) and conducted a moving-window average analysis on the hourly T_c and T_a time-series data, respectively, with the window size equal to the sample number (n=24 hours; we resampled all flux data to hourly intervals) of each day. The moving-window-averaged T_c (T_{c_MA}) and T_a (T_{a_MA}) as a result of this step (i.e., the conceptual line shown in Fig. 4a-iii) only contains the seasonal information. By subtracting T_{c_MA} and T_{a_MA} from their original

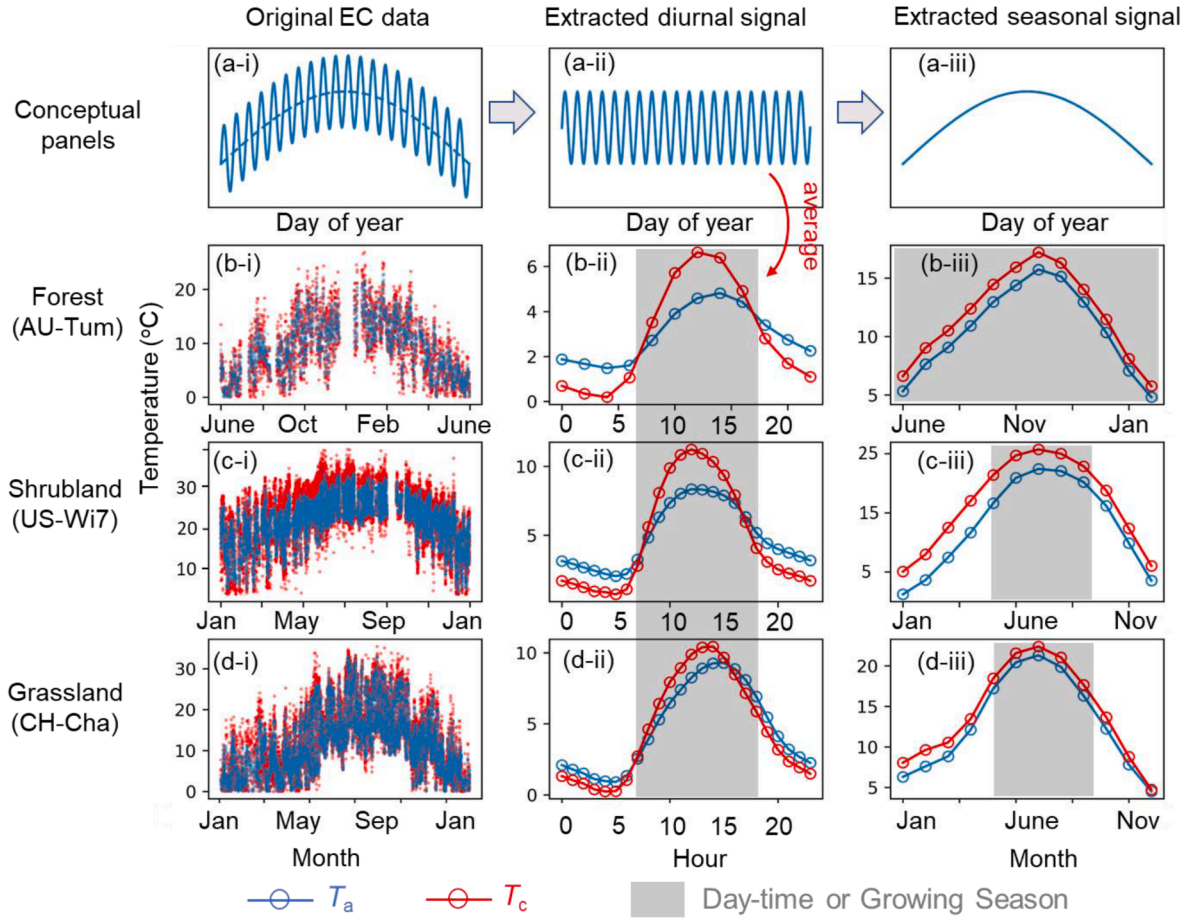

Fig. 4. Partitioning the time-series of hourly air (T_a) and canopy (T_c) temperature into the diurnal and seasonal signals using eddy covariance flux measurements. Panel (a) displays the conceptual time-series dynamics on an annual cycle (a-i) that can be further partitioned to the signals on the diurnal (a-ii) and seasonal (a-iii) timescales, respectively. Panel (b-d) displays the examples of the three real-world vegetated ecosystems, including (b) a forest site of AU-Tum (35.66° S, 148.15° E), with a mean growing-season LAI of 5.2 m^2/m^2; (c) a shrubland site of US-Wi7 (49.65° N, 91.07° W), with a mean growing-season LAI of 3.6 m^2/m^2; and (d) a grassland site of CH-Cha (47.21° N, 8.41° W), with a mean growing-season LAI of 2.9 m^2/m^2. From left to right, the panels illustrate the results of (i) original, (ii) diurnal, and (iii) seasonal data.

hourly T_c and T_a data, it is possible to derive residual data that only includes diurnal information (Fig. 4a-ii; Tiwariet al., 2013). Step 2—deriving PTC at hourly and seasonal timescales. Here we followed Guo et al. (2023) and only focused on the T_c *vs.* T_a relationship during those daytime observations when photosynthetically active radiation (PAR) is over 100 μmol m^{-2} s^{-1}. This is because the night-time T_c *vs.* T_a relationship can be mainly driven by physical processes like radiative cooling (Jones, 2013; Guo et al., 2022) and thus does not reflect the full picture of PTC that is subject to both abiotic and biotic controls. With the above-derived diurnal and seasonal data (including daytime observations only), we calculated the regression slope of T_c *vs.* T_a to derive the corresponding PTC on both timescales of interest. In addition, we further compared the diurnal *vs*. seasonal PTC patterns for different PFTs.

2.3.3. Exploring the mechanisms underlying thermoregulation differences between diurnal and seasonal timescales

To answer question 2 (what are the mechanisms underlying the differences between diurnal and seasonal PTC?), we compared diurnal *vs*. seasonal differences in the key processes that regulate plant thermodynamics. For plants, their canopies are often warmer than air during the middy due to high solar radiation (Jones, 2013; Guo et al., 2023; Still et al., 2022). Therefore, to avoid extremely high tissue temperatures, plants usually thermoregulate to reduce absorbed net energy (R_n) and/or enhance transpiration cooling (latent heat; *LE*) and canopy-to-air convection (related to sensible heat, *H*). Because T_c is mainly determined by the balance of R_n, *LE*, and *H* ($R_n = H + LE +$ G, here G is stored energy by soil, which usually is proportional to R_n; Jones, 2013), we compared how *LE* and *H* respond to R_n change between diurnal and seasonal timescales.

We expected that as R_n increases, if more absorbed energy is used for transpiration cooling (converted to *LE*), this means that less energy was converted to *H*, which will result in a smaller positive canopy-to-air temperature difference (ΔT) (Fig. S3). [Notably, a higher *H* may not increase ΔT if aerodynamic conductance for heat exchange (G_H) increases simultaneously (Muller et al., 2023). However, we did not analyze the impact of G_H due to a lack of necessary plant trait information for G_H calculation.] Specifically, we used *LE* (and *H*) *vs.* R_n slope to indicate the relative change of *LE* (and *H*) to R_n. A larger *LE vs.* R_n (or smaller *H vs.* R_n) slope indicates that more R_n converted to *LE* and less to *H*, resulting in a slower warming rate for plants (i.e. smaller T_c *vs.* T_a slope). Our pre-analysis based on observations of 155 flux sites confirms this pattern, showing that sites with larger *LE vs.* R_n slopes have smaller T_c *vs.* T_a slopes (Fig. S4a,b), and *LE* (or *H*) *vs.* R_n slope correlates better with PTC than *LE* or *H* alone (Fig. S4c,d).

2.3.4. Exploring the drivers of global spatial PTC variability across both diurnal and seasonal timescales

To answer question 3 (What are the drivers of spatial variability in plant thermoregulation capability across the two timescales of interest?), we used a tree-based machine learning model (eXtreme Gradient Boosting, XGB; Chen et al., 2015) coupled with the SHapley Additive exPlanations (SHAP) framework (Lundberg et al., 2020) to explore the contribution of each biotic and abiotic variable to the variability of PTC across sites. The XGB model is a nonlinear model, which has been widely used for local interpretations in the SHAP framework (Valavi et al., 2022; Wang et al., 2022; Zhang et al., 2021). The SHAP method is based on the Shapley value concept from game theory (Lundberg & Lee, 2017), which directly monitors the impacts of individual features (e.g., those abiotic and biotic variables) on model loss using the differences between the model predicted and expected values (Lundberg et al., 2020). Specifically, the predicted value is the output of the XGB model with all features as inputs, while the expected value is the mean of the output obtained from all combinations of features other than the target feature. A higher difference indicates greater feature importance. The average of the absolute SHAP values is viewed as the SHAP feature importance of a certain variable.

18 abiotic and biotic variables showing direct linkages with the energy balance process were used as explanatory variables (details are shown in Table 1). These variables were derived from FLUXNET, satellite, and re-analysis products following the standard methods (also see Section 2.2 above), including T_a, RH, elevation, *u, u**, VPD, SWC, PAR, precipitation (P), LAI, water availability (indicated by actual ET/potential ET ratio), Hc, water use efficiency (WUE, indicated by GPP/ET ratio), PFT, *LE, H*, the *LE vs.* R_n regression slope, and the *H vs.* R_n regression slope. To minimize collinearity among these variables, we calculated the correlation between each of the two variables and found that some variables are highly correlated, such as VPD with T_a and *LE* with PAR (Fig. S5a). We thus removed those highly correlated variables, including VPD, *LE, H*, and the *H vs.* R_n slope from the following analysis. The remaining variables exhibited $R^2 < 0.44$ (Fig. S5b). The analysis includes two steps. First is model development and validation. We calibrated and evaluated the XGB model ('xgboost' package in Python) across all global sites with the above 14 variables being model inputs and the slope of T_c *vs.* T_a being the model output. The model displayed a satisfactory performance with an R^2 above 0.5 for leave-one-out cross-validation (Fig. S7). The second is feature importance (SHAP values) calculation. We applied the SHAP method ('shap' package in Python) to detect each variable's effect on the slope of T_c *vs.* T_a, which is indicated by the SHAP values of each variable. Notably, the above analyses were conducted on the diurnal and seasonal timescale, respectively.

3. Results

3.1. Question 1: Diurnal vs. seasonal thermoregulation capability

Our results show that T_c is linearly correlated with T_a at both diurnal and seasonal timescales, showing very high average R^2: 0.84 for diurnal data and 0.92 for seasonal data. However, slopes of T_c *vs.* T_a are significantly larger ($p<0.001$ for paired t-test) at diurnal (mean: 1.18) than seasonal (mean: 0.98) timescales, meaning that T_c changes faster with T_a at the diurnal timescale and thus indicating a significantly stronger seasonal thermoregulation capability (Fig. 5). Among all examined EC flux sites around the world, diurnal T_c *vs.* T_a slopes vary largely from 0.9 to 1.8, with 80% of all sites having slopes>1.1 (megathermy), 19% of all sites having slopes 0.9-1.1 (poikilothermy), and 1% of all sites having slopes<0.9 (limited homeothermy) (Fig. 5a). The seasonal T_c *vs.* T_a slopes, by contrast, have a smaller variation range from 0.8 to 1.3, with 40% of all sites having slopes>1.1, 41% of all sites having slopes 0.9-1.1, and 19% of all sites having slopes<0.9 (Fig. 5b).

To further assess whether the PTC difference between the two timescales of diurnal and seasonal is persistent within and across PFTs, we aggregated those sites belonging to the same PFT. Regardless of the PFTs being analyzed, i.e., forest, grassland, shrubland, savanna, cropland, and wetland, our results show that the diurnal slopes are significantly larger than the seasonal slopes (Fig. 5c).

3.2. Question 2: Underlying mechanisms of thermoregulation differences between diurnal and seasonal timescales

Our results demonstrate a significant difference in the response of *LE* and *H* to R_n between the diurnal and seasonal timescales, with *LE* increasing faster at the seasonal timescale, while *H* increasing faster at the diurnal timescale. Specifically, we observed a larger slope of *LE* against R_n at the seasonal timescale (slope: 0.47) than at the diurnal timescale (slope: 0.41), indicating transpiration cooling increases faster at the seasonal timescale (Fig. 6b). Conversely, for *H*, we observed an opposite trend, with the diurnal slope being larger (0.49) than the seasonal slope (0.45). The stronger transpiration cooling response at the seasonal timescale resulted in a smaller increase in ΔT on the seasonal timescale (slope: 0.0017) than on the diurnal timescale (slope: 0.0034) for the same increase in R_n (Fig. 6c), which helps explain why T_c increases more slowly at the seasonal timescale, as shown in Fig. 5.

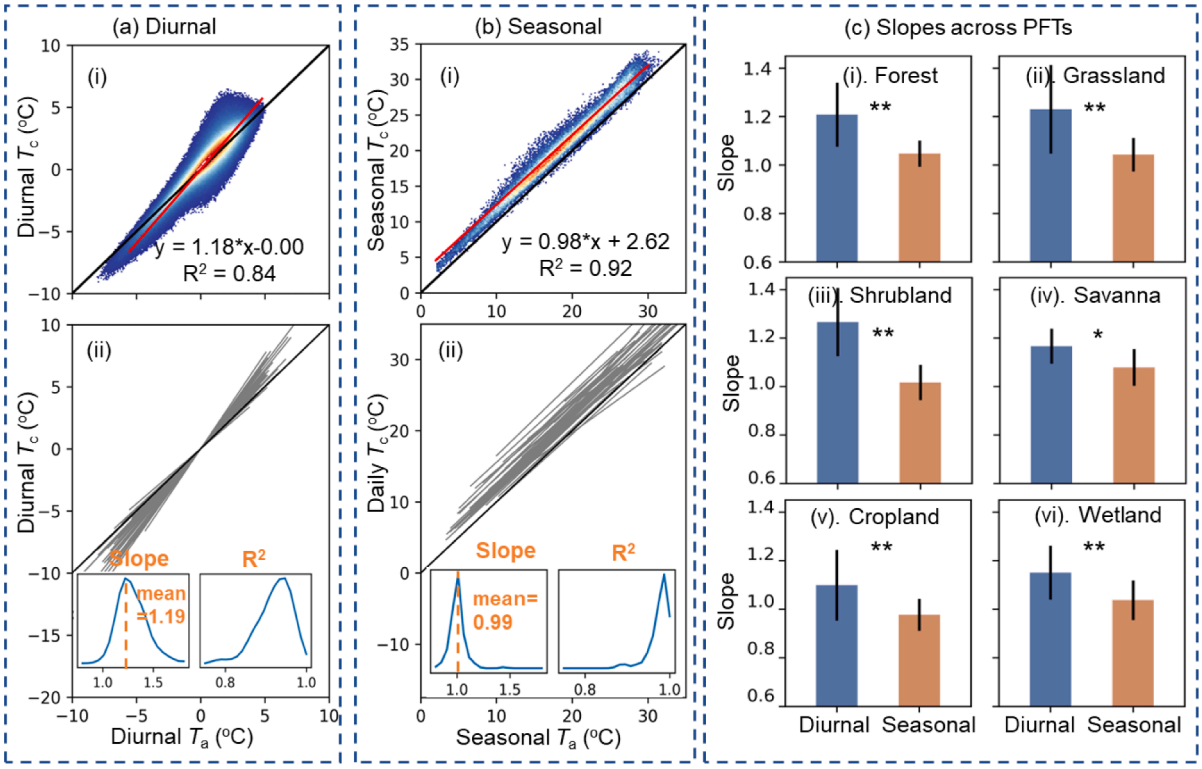

Fig. 5. Diurnal and seasonal relationships of the plant canopy (T_c) *vs.* air (T_a) temperature displayed at the site and PFT level. Temporal-scale regressions of T_c *vs.* T_a across diurnal (a) and seasonal (b) timescales using EC data, including (i) fitted results derived from data across all available sites (n=155); (ii) fitted results for each EC site, where each grey line corresponds to each site, histograms indicate frequency distributions of regression slope and R^2, the orange dashed line is the mean of the slope. (c) The slope indicators for each site were grouped by PFT. The error bar indicates 1 standard deviation; * and ** refer to p<0.05 and 0.01 of paired t-test, respectively.

To further explore the reason for the different transpiration responses at the diurnal and seasonal timescale, we compared LE_{norm} (i.e. $LE \times \frac{\partial T_a}{\partial R_n}$, indicating LE normalized by R_n, see Method S1 for details) *vs.* T_a relationships between the two timescales (Fig. 7). We found that the different transpiration responses across the two timescales are mainly induced by the different responses of LE_{norm} to high T_a: at the diurnal timescale, LE_{norm} firstly increases with T_a, peaks at around intermediate T_a (blue dashed line in Fig. 7a), and then decreases afterwards; at the seasonal timescale, LE_{norm} always increases with T_a (orange line in Fig. 7a). In other words, transpiration cooling works in a wider temperature range at seasonal than diurnal timescale (evident also by the larger slope of LE_{norm} to T_a at seasonal timescale; panel a-ii of Fig. 7). The findings are consistent across all six PFTs examined (Fig. 7b), including forest, grassland, shrubland, savanna, cropland, and wetland.

3.3. *Question 3: The relative contribution of each abiotic and biotic variable to the spatial variability in plant thermoregulation capability*

To assess the relative importance of each abiotic and biotic variable in driving the large spatial PTC variability (Fig. S6), we utilized the XGB-SHAP modeling framework. The resulting XGB models for the diurnal and seasonal timescale explained 53% and 51% of the global PTC variability, respectively (Fig. S7a,b). By applying the SHAP framework to these models, we obtained the rank importance of each variable (Fig. 8b,c,d,e). Among the 14 variables examined, the *LE vs.* R_n slope and water availability (indicated by the ratio of actual ET and potential ET), display the highest and second highest explanatory power on the global PTC variability, consistently across both diurnal (Fig. 8b) and seasonal (Fig. 8e) timescales. However, we also noted that the importance of other variables varies considerably between the two timescales (Fig. 8b, e). Focusing on the two most important variables (the *LE vs.* R_n slope and water availability; Fig. 8c,f), we found both variables to exhibit significant, negative relationships with PTC, indicating that higher *LE vs.* R_n slope and greater water availability tend to increase the cooling effect, thus enhancing the PTC (leading to lower slopes of T_c *vs.* T_a).

4. Discussion

Plant canopy temperature (T_c) plays an important role in affecting plant growth as it tightly and non-linearly regulates the rates of plant photosynthesis, respiration, and transpiration (Still et al., 2021; Huang et al., 2019). Despite having evidence that the dominant drivers responsible for T_c depend on the timescale of interest (Jones, 2013; and our Fig. 1b), it has not been assessed whether they would result in distinct plant thermoregulation capabilities (PTCs) across different timescales. This knowledge gap poses a concern regarding whether the short-term findings related to PTC (based on diurnal observations) can be extended to longer-term predictions (season and beyond). Previous studies on the PTC effect were conducted at different timescales and have reported contradictory results (Fauset et al., 2018; Miller et al., 2021; Still et al., 2022). For example, relying on diurnal observations made across several days from infrared thermal sensors in a subtropical evergreen forest, Fauset et al (2018) evaluated the T_c *vs.* T_a relationship and found that upper canopies usually show megathermy thermoregulation patterns (i.e., the slope of T_c *vs.* T_a is above 1). Later, Drake et al (2020) examined the same issue but using much longer time-series observations, and found much smaller regression slopes of T_c *vs.* T_a close to 1. Such reported thermoregulation differences across studies may be the results of the variation of PTC across timescales (e.g. diurnal observations in Fauset et al (2018) *vs.* mixed timescale observations of both diurnal and seasonal in Drake et al (2020)). Furthermore, a synthesis study helps to examine the PTC issue across a wide range of forest types

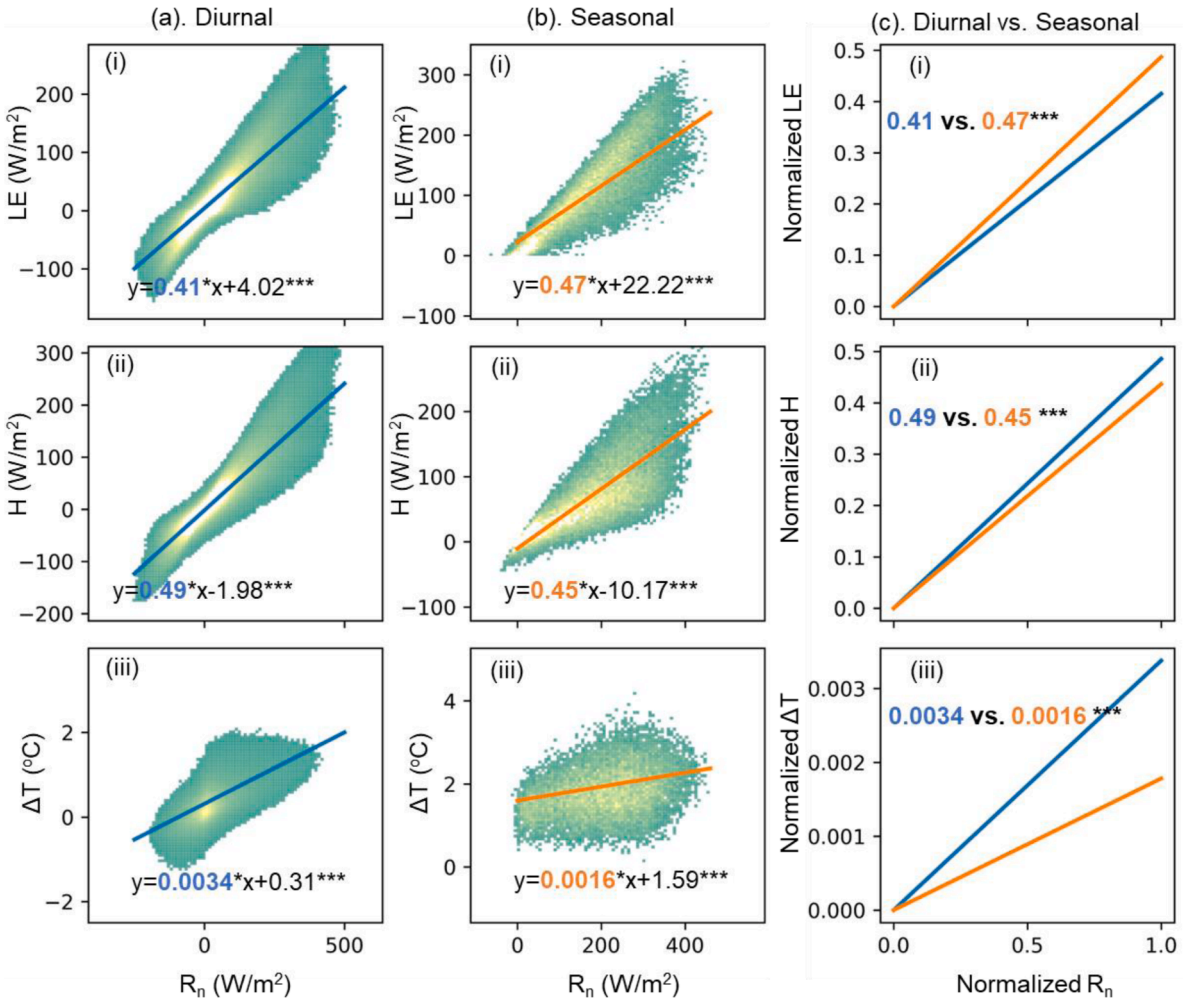

Fig. 6. The responses of (i) latent heat (*LE*), (ii) sensible heat (*H*), and (iii) canopy-to-air temperature (ΔT) to increasing net absorbed radiation (R_n) at the diurnal and seasonal timescale, respectively. Panel (a) shows the diurnal relationship, while panel (b) shows the seasonal relationship. Panel (c) presents a comparison between the diurnal and seasonal relationships. "***" represents a p-value less than 0.001.

and climate zones (Still et al., 2022), while whether similar findings can be extended to other vegetated ecosystems around the world remain unknown.

Using the global eddy flux dataset (n=155 sites) covering all major PFTs around the world, we found that PTC (indicated by the regression slope between timeseries of T_c and T_a) is significantly smaller at the seasonal than the diurnal timescale, at both site and PFT levels. This finding indicates a slower change in T_c with a given change in T_a (and thus implies a stronger PTC) at the seasonal timescale (Fig. 5), which has important implications for broader thermal ecology studies. First, our study largely expanded the ecosystem types and regions for PTC hypothesis testing. Previously, the 'limited homeothermy' hypothesis (Mahan and Upchurch, 1988; Michaletz et al., 2016) has often been used to describe PTC, but was only tested from limited experimental data of crop plants (Still et al., 2019; Cook et al., 2021) or from limited natural plant canopies/ecosystems (Drake et al., 2020; Still et al., 2022). By expanding the scale of the study to the globe and including multiple ecosystem types (i.e. forest, grassland, shrubland, savanna, cropland, and wetland), our study helps to reconcile diverse PTC patterns observed previously ranging from no (Drake et al., 2020; Still et al., 2022) to moderate (Blonder & Michaletz et al., 2018; Cook et al., 2021) PTC. Our results demonstrated that plant ecosystems indeed exhibit diverse PTC patterns across the globe with the T_c *vs.* T_a regression slope changing from 0.7-1.3, implying that these divergent results reported previously may not be incompatible. Instead, they could be caused by different biotitic and abiotic conditions.

Secondly, our finding of stronger PTC at the seasonal than the diurnal timescale implies that plants may deal better with slow, gradual temperature change (from day to day along seasons) than rapid, short-term temperature change (large diurnal fluctuations within a day). The potential reason for this may be that plants cannot avoid extreme heat by changing their leaf shape or branch orientation at the short timescale (i.e., diurnal). Whereas on the seasonal scale, plants have abilities to change these at a slow rate in line with the seasonal changes of environmental conditions (e.g. soil water content and solar radiation), which helps reduce the solar radiation received or increase the rate of heat diffusion and transpiration, leading to enhanced cooling (Jones, 2013; Muller et al., 2021; Muller et al., 2023). Consequently, we expect that short-term temperature extremes (e.g., the anomaly aspect of climate change) may put more stress on plant functioning and health than long-term, gradual temperature increases (e.g., the mean trend of climate change). This implication seems to support recent large-scale observations that increasing the frequency and intensity (on average, 8 days/year during the 1960s to 20 days/year during the 2010s) of heat waves leads to significant negative impacts (up to -34% compared to no heatwave) on regional plant productivity and terrestrial photosynthetic carbon uptake (Perkins-Kirkpatrick & Lewis, 2020; Ainsworth & Long, 2021; Breshears et al., 2021). Finally, due to the PTC difference between diurnal and seasonal timescales (Fig. 5-7), one should be wary of extending the conclusion drawn from short-term observations to

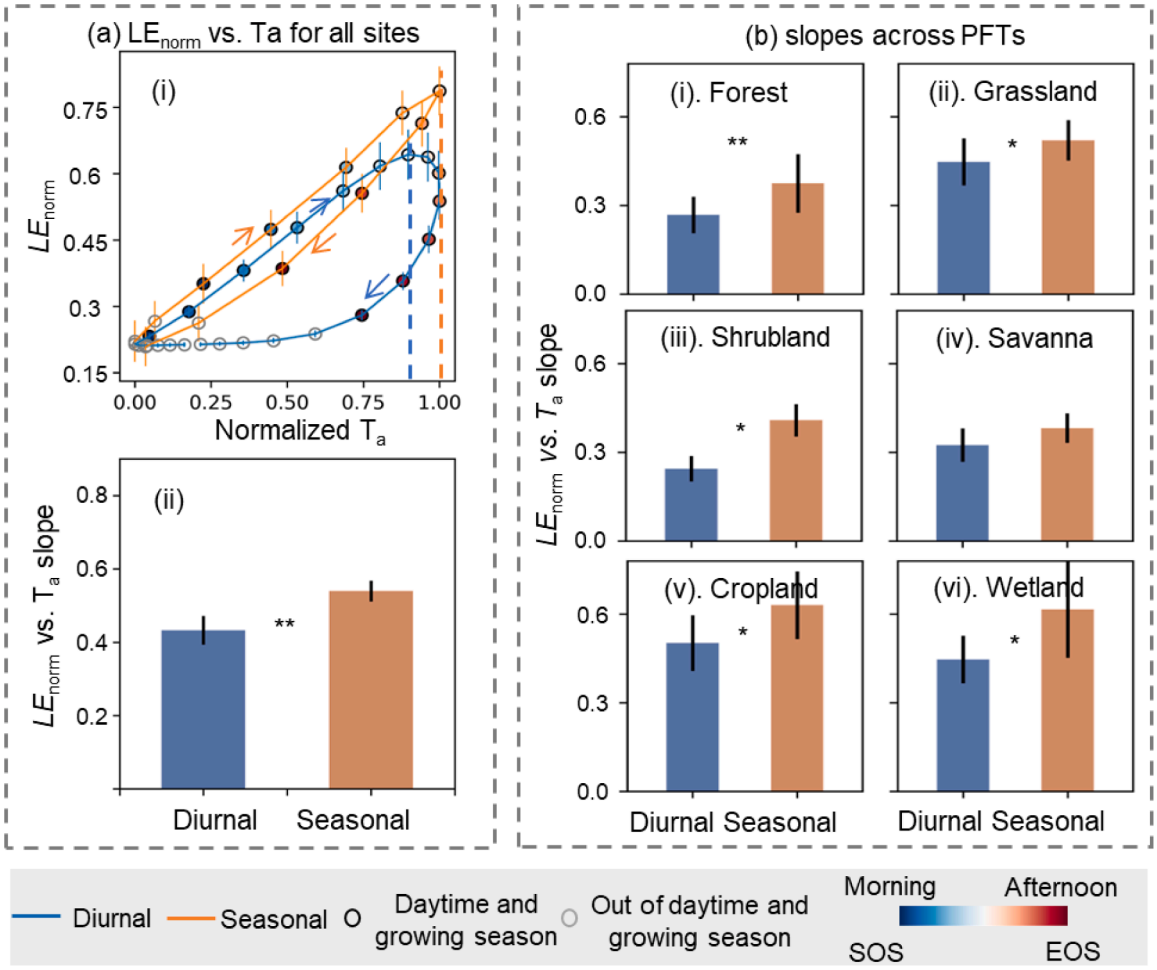

Fig. 7. Diurnal and seasonal relationships of normalized transpiration rate (LE_{norm}) response to air temperature (T_a). (a) The LE_{norm} *vs.* T_a relationship at the diurnal (blue line; each circle indicates one hour) and seasonal (orange line; each circle indicates one month) timescale, which is derived based on the data from all flux sites (n=155). (b) Site-level linear regression slopes of LE_{norm} *vs.* T_a are subsequently grouped into each PFT. The error bar indicates 1 standard deviation; * and ** refer to p<0.05 and 0.01 of paired t-test, respectively. SOS and EOS refer to the start and end of the growing season.

longer-term predictions. If ignoring the difference between timescales, we may generate inaccurate predictions in canopy temperatures and other metabolic processes dependent on canopy temperature (Farella et al., 2022; Still et al., 2022).

Furthermore, we explored how transpiration cooling (*LE*) and canopy-to-air convection (*H*) respond to R_n, and found that *LE* increases faster (but *H* increases slower) at the seasonal timescale (Fig. 6). This is caused by the different *LE* responses to high T_a between the two timescales, with a convex relationship at the diurnal timescale and a monotonous, positive relationship at the seasonal timescale (Fig. 7). This finding is novel, but also agrees with the fundamental plant ecophysiology and energy balance principles that more transpiration cooling usually leads to cooler T_c (Campbell and Norman, 2012; Mohr and Schopfer, 2012; Wu et al., 2020). Within a day, plant canopies tend to initially increase their transpiration rates with T_a (and solar radiation) and then down-regulate their stomata around midday when T_a (and VPD) is very high (above ~85th percentile of T_a) for water conservation, causing a negative relationship between transpiration and T_a (blue line in Fig. 7-i) (Medlyn et al., 2011; Vialet-Chabrand et al., 2013; Matthews et al., 2018). While at the seasonal scale, the hottest period tends to occur during the peak growing season, which often comes with sufficient precipitation (Pascale et al., 2015), resulting in sufficient water supply for plant transpiration cooling, despite a high T_a (orange line in Fig. 7-i). Such different LE_{norm} *vs.* T_a relationships across timescales, explain why *LE* increases faster with R_n (and PTC is stronger) at the seasonal than the diurnal timescale (Fig. 5,6).

Additionally, we observed large spatial PTC variability across different plant ecosystems, but no clear trends along the temperature and precipitation gradient (Fig. S6), which may imply that T_a and precipitation are not the dominant drivers of spatial PTC variability. To allow for a more holistic understanding of abiotic and biotic controls of spatial PTC variability, we further compiled a comprehensive list of candidate variables (n=14). We found that the slope of *LE vs.* R_n has the highest explanatory power for PTC for both diurnal and seasonal timescales (Fig. 8). It is because energy allocation (i.e. how many fractions of energy absorbed is used for *LE* or *H*) importantly regulates T_c. If more energy is used for transpiration cooling (LE) and less for *H*, plants will have a slower warming rate with absorbed energy increasing (Fig. 6,7, S3; Jones, 2013). Water availability (indicated by ET/PET ratio) also importantly regulates PTC (Fig. 8c), suggesting that ample water availability is essential to sustain plant transpiration cooling and health (Jones, 2013; Zhang et al., 2019; 2022). This implies that future changes in precipitation and associated transpiration cooling will have an important impact on PTC, with areas of increased precipitation likely to have higher PTC, while the opposite will be true for areas with reduced precipitation. Additionally, non-transpiration cooling associated with sensible heat and aerodynamic conductance remains an important topic for future work (Rotenberg & Yakir., 2010; Leigh et al., 2017; Muller et al. 2021), especially considering that atmospheric dryness will increase in the future (Yuan et al., 2019; Breshears et al., 2021).

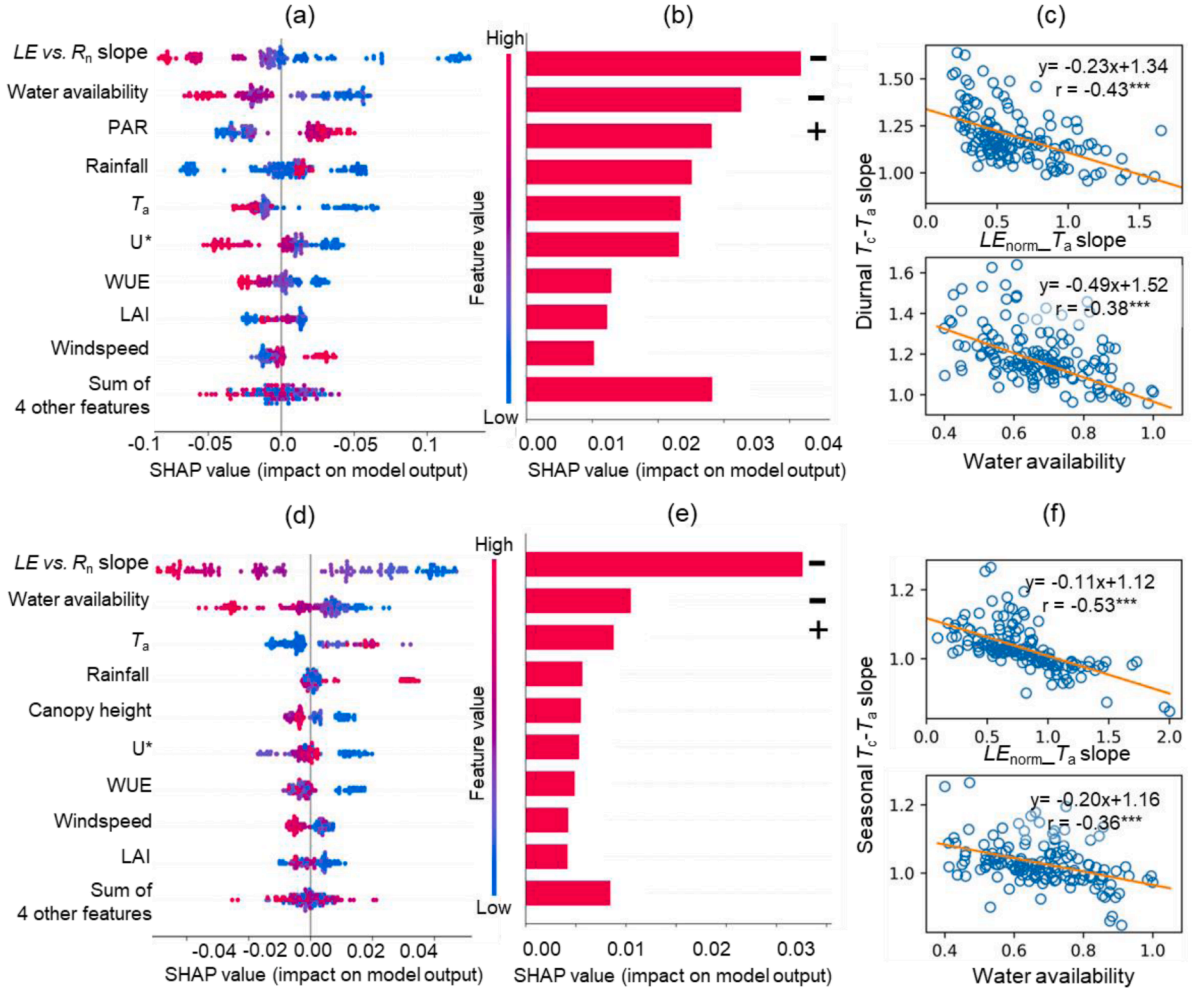

Fig. 8. The relative variable contribution to the global plant thermoregulation capability (PTC, indicated by the site-specific regression slope of T_c *vs.* T_a) variability at the diurnal (a-c) and seasonal (d-f) timescale, respectively. In panels a&d, one point indicates one site, and color represents the feature value (red high, blue low), and positive (negative) SHAP values refer to the positive (negative) impact on model outputs. In panels b&e, the relative variable importance is assessed using the mean SHAP values, a higher value mean that the feature is more important; (c&e) the paired relationships between the two most important variables and PTC were displayed at diurnal and seasonal timescale, respectively. The '+' and '−' in panels b&e indicate the feature is positively and negatively partially correlated with plant thermoregulation capabilities. *** refer to $p<0.001$ of paired t-test.

5. Conclusion

To understand how plant thermoregulation capability varies across different timescales, we extracted diurnal and seasonal signals of T_c, T_a, and other relevant variables from hourly flux data, and then compared thermoregulation patterns between the two timescales. We found that plant canopies exhibit different thermoregulation capabilities between the two timescales, with significantly higher thermoregulation capability at the seasonal than the diurnal timescale. Further, we revealed that this difference is mainly caused by the difference in transpiration response between the two timescales (i.e., the convex response at the diurnal timescale *vs.* the positive, monotonous response at the seasonal timescale). Finally, we explored the drivers of the spatial variability in plant thermoregulation capability across the global flux sites and found that the *LE vs.* R_n slope and water availability (indicated by the ET/PET ratio) are the two most important explanatory variables. These results altogether suggest that caution is needed when expanding conclusions for short-term observational PTC studies to longer-term predictions and *vice versa*.

Author contributions

Z.G. conceived and designed the study with significant inputs from J. W. Z.G. performed the analyses. All authors contributed to interpreting the results. Z.G. wrote the first draft of the paper and all authors contributed to editing and revising the manuscript.

Declaration of Competing Interest

None.

Data availability

Data will be made available on request.

Acknowledgments

We thank the reviewers for their constructive suggestions. We thank FLUXNET, Asiaflux, European flux, and Brazil flux for data support. We also thank Prof. Shuli Niu for her kind assistance in accessing Asiaflux data. This work was supported by the National Natural Science

Foundation of China (#31922090), Hong Kong Research Grants Council Early Career Scheme (#27306020). J.W. was supported by the HKU Seed Funding for Strategic Interdisciplinary Research Scheme, the Hung Ying Physical Science Research Fund 2021-22, and the Innovation and the Innovation and Technology Fund (funding support to State Key Laboratories in Hong Kong of Agrobiotechnology) of the HKSAR, China. C.K.F.L. was in part supported by the HKU seed fund for basic research (#202011159154) and the HKU 45th round PDF scheme. C.J.S. was supported by the US National Science Foundation (awards 1802885 and 1926431).

Supplementary materials

Supplementary material associated with this article can be found, in the online version, at doi:10.1016/j.agrformet.2023.109582.

References

Ainsworth, E.A., Long, S.P., 2021. 30 years of free-air carbon dioxide enrichment (FACE): what have we learned about future crop productivity and its potential for adaptation? Global Change Biology 27 (1), 27–49.
Blonder, B., Michaletz, S.T., 2018. A model for leaf temperature decoupling from air temperature. Agricultural and Forest Meteorology 262, 354–360.
Blonder, B., Escobar, S., Kapás, R.E., Michaletz, S.T., 2020. Low predictability of energy balance traits and leaf temperature metrics in desert, montane and alpine plant communities. Functional Ecology 34 (9), 1882–1897.
Breshears, D.D., Fontaine, J.B., Ruthrof, K.X., Field, J.P., Feng, X., Burger, J.R., Law, D.J., Kala, J., Hardy, G.E.S.J., 2021. Underappreciated plant vulnerabilities to heat waves. New Phytologist 231 (1), 32–39.
Campbell, G.S., Norman, J.M., 2012. An introduction to environmental biophysics. Springer Science & Business Media.
Chen, T., He, T., Benesty, M., Khotilovich, V., Tang, Y., Cho, H., Chen, K., 2015. Xgboost: extreme gradient boosting. R package version 0.4-2 1 (4), 1–4.
Cook, A.M., Berry, N., Milner, K.V., Leigh, A., 2021. Water availability influences thermal safety margins for leaves. Functional Ecology 35 (10), 2179–2189.
Dong, N., Prentice, I.C., Harrison, S.P., Song, Q.H., Zhang, Y.P., 2017. Biophysical homoeostasis of leaf temperature: A neglected process for vegetation and land-surface modelling. Global Ecology and Biogeography 26 (9), 998–1007.
Doughty, C.E., Goulden, M.L., 2008. Are tropical forests near a high temperature threshold? Journal of Geophysical Research: Biogeosciences 113 (G1).
Drake, J.E., Harwood, R., Vårhammar, A., Barbour, M.M., Reich, P.B., Barton, C.V., Tjoelker, M.G., 2020. No evidence of homeostatic regulation of leaf temperature in Eucalyptus parramattensis trees: integration of CO2 flux and oxygen isotope methodologies. New Phytologist 228 (5), 1511–1523.
Ehleringer, J.R., Forseth, I.N., 1989. Diurnal leaf movements and productivity in canopies. Plant canopies: their growth, form and function 31, 129–142.
Farella, M.M., Fisher, J.B., Jiao, W., Key, K.B., Barnes, M.L., 2022. Thermal remote sensing for plant ecology from leaf to globe. Journal of Ecology 110 (9), 1996–2014.
Fauset, S., Freitas, H.C., Galbraith, D.R., Sullivan, M.J., Aidar, M.P., Joly, C.A., Phillips, O.L., Vieira, S.A., Gloor, M.U., 2018. Differences in leaf thermoregulation and water use strategies between three co-occurring Atlantic forest tree species. Plant, cell & environment 41 (7), 1618–1631.
Friedl, M, Sulla-Menashe, D., 2015. MCD12Q1 MODIS/Terra+ aqua land cover type yearly L3 global 500m SIN grid V006 [data set]. NASA EOSDIS Land Processes DAAC 10, 200.
Gates, D.M., Alderfer, R., Taylor, E., 1968. Leaf temperatures of desert plants. Science 159 (3818), 994–995.
Gorelick, N., Hancher, M., Dixon, M., Ilyushchenko, S., Thau, D., Moore, R., 2017. Google Earth Engine: Planetary-scale geospatial analysis for everyone. Remote sensing of Environment 202, 18–27.
Guo, Z., Still, C.J., Lee, C.K., Ryu, Y., Blonder, B., Wang, J., Bonebrake, T.C., Hughes, A., Li, Y., Yeung, H.C., Zhang, K., 2023. Does plant ecosystem thermoregulation occur? An extratropical assessment at different spatial and temporal scales. New Phytologist 238 (3), 1004–1018.
Guo, Z., Yan, Z., Majcher, B.M., Lee, C.K., Zhao, Y., Song, G., Wang, B., Wang, X., Deng, Y., Michaletz, S.T., Ryu, Y., 2022. Dynamic biotic controls of leaf thermoregulation across the diel timescale. Agricultural and Forest Meteorology 315, 108827.
Guillevic, P., Göttsche, F., Nickeson, J., Hulley, G., Ghent, D., Yu, Y., Trigo, I., Hook, S., Sobrino, J.A., Remedios, J., Román, M., 2018. Land surface temperature product validation best practice protocol. version 1.1. Best Practice for Satellite-Derived Land Product Validation 60.
Helliker, B.R., Richter, S.L., 2008. Subtropical to boreal convergence of tree-leaf temperatures. Nature 454 (7203), 511–514.
Huang, M., Piao, S., Ciais, P., Peñuelas, J., Wang, X., Keenan, T.F., Peng, S., Berry, J.A., Wang, K., Mao, J., Alkama, R., 2019. Air temperature optima of vegetation productivity across global biomes. Nature ecology & evolution 3 (5), 772–779.
Jin, J., Yan, T., Wang, H., Ma, X., He, M., Wang, Y., Wang, W., Guo, F., Cai, Y., Zhu, Q., Wu, J., 2022. Improved modeling of canopy transpiration for temperate forests by incorporating a LAI-based dynamic parametrization scheme of stomatal slope. Agricultural and Forest Meteorology 326, 109157.
Jones, H.G., 2013. Plants and microclimate: a quantitative approach to environmental plant physiology. Cambridge university press.
Knauer, J., Zaehle, S., Medlyn, B.E., Reichstein, M., Williams, C.A., Migliavacca, M., De Kauwe, M.G., Werner, C., Keitel, C., Kolari, P., Limousin, J.M., 2018. Towards physiologically meaningful water-use efficiency estimates from eddy covariance data. Global Change Biology 24 (2), 694–710.
Lang, N, Jetz, W, Schindler, K, Wegner, JD., 2022. A high-resolution canopy height model of the Earth. arXiv preprint arXiv:2204.08322.
Leigh, A., Sevanto, S., Close, J.D., Nicotra, A.B., 2017. The influence of leaf size and shape on leaf thermal dynamics: does theory hold up under natural conditions? Plant, cell & environment 40 (2), 237–248.
Leuzinger, S., Körner, C., 2007. Tree species diversity affects canopy leaf temperatures in a mature temperate forest. Agricultural and forest meteorology 146 (1-2), 29–37.
Lin, H., Tu, C., Fang, J., Gioli, B., Loubet, B., Gruening, C., Zhou, G., Beringer, J., Huang, J., Dušek, J., Liddell, M., 2020. Forests buffer thermal fluctuation better than non-forests. Agricultural and Forest Meteorology 288, 107994.
Lundberg, S.M., Lee, S.I., 2017. A unified approach to interpreting model predictions. Advances in neural information processing systems 30.
Lundberg, S.M., Erion, G., Chen, H., DeGrave, A., Prutkin, J.M., Nair, B., Katz, R., Himmelfarb, J., Bansal, N., Lee, S.I., 2020. From local explanations to global understanding with explainable AI for trees. Nature machine intelligence 2 (1), 56–67.
Mahan, J.R., Upchurch, D.R., 1988. Maintenance of constant leaf temperature by plants—I. Hypothesis-limited homeothermy. Environmental and Experimental Botany 28 (4), 351–357.
Matthews, J.S., Vialet-Chabrand, S., Lawson, T., 2018. Acclimation to fluctuating light impacts the rapidity of response and diurnal rhythm of stomatal conductance. Plant Physiology 176 (3), 1939–1951.
Medlyn, B.E., Duursma, R.A., Eamus, D., Ellsworth, D.S., Prentice, I.C., Barton, C.V., Crous, K.Y., De Angelis, P., Freeman, M., Wingate, L., 2011. Reconciling the optimal and empirical approaches to modelling stomatal conductance. Global Change Biology 17 (6), 2134–2144.
Michaletz, S.T., Weiser, M.D., Zhou, J., Kaspari, M., Helliker, B.R., Enquist, B.J., 2015. Plant thermoregulation: energetics, trait–environment interactions, and carbon economics. Trends in ecology & evolution 30 (12), 714–724.
Michaletz, S.T., Weiser, M.D., McDowell, N.G., Zhou, J., Kaspari, M., Helliker, B.R., Enquist, B.J., 2016. The energetic and carbon economic origins of leaf thermoregulation. Nature plants 2 (9), 1–9.
Miller, B.D., Carter, K.R., Reed, S.C., Wood, T.E., Cavaleri, M.A., 2021. Only sun-lit leaves of the uppermost canopy exceed both air temperature and photosynthetic thermal optima in a wet tropical forest. Agricultural and Forest Meteorology 301, 108347.
Mohr, H., Schopfer, P.eds., 2012. Plant physiology. Springer Science & Business Media.
Muller, J.D., Rotenberg, E., Tatarinov, F., Oz, I., Yakir, D., 2021. Evidence for efficient nonevaporative leaf-to-air heat dissipation in a pine forest under drought conditions. New Phytologist 232 (6), 2254–2266.
Muller, J., Rotenberg, E., Tatarinov, F., Oz, I., Yakir, D., 2023. Detailed in-situ leaf energy budget permits the assessment of leaf aerodynamic resistance as a key to enhance non-evaporative cooling under drought. Plant, cell & environment. https://doi.org/10.1111/pce.14571.
Muñoz-Sabater, J., Dutra, E., Agustí-Panareda, A., Albergel, C., Arduini, G., Balsamo, G., Boussetta, S., Choulga, M., Harrigan, S., Hersbach, H., Martens, B., 2021. ERA5-Land: A state-of-the-art global reanalysis dataset for land applications. Earth System Science Data 13 (9), 4349–4383.
Myneni, R, Knyazikhin, Y, Park, T., 2015. MCD15A3H MODIS/Terra+ Aqua Leaf Area Index/FPAR 4-day L4 Global 500 m SIN Grid V006 [data set]. NASA EOSDIS Land Processes DAAC.
Pascale, S., Lucarini, V., Feng, X., Porporato, A., 2015. Analysis of rainfall seasonality from observations and climate models. Climate Dynamics 44 (11), 3281–3301.
Pastorello, G., Trotta, C., Canfora, E., Chu, H., Christianson, D., Cheah, Y.W., Poindexter, C., Chen, J., Elbashandy, A., Humphrey, M., Isaac, P., 2020. The FLUXNET2015 dataset and the ONEFlux processing pipeline for eddy covariance data. Scientific data 7 (1), 1–27.
Pau, S., Detto, M., Kim, Y., Still, C.J., 2018. Tropical forest temperature thresholds for gross primary productivity. Ecosphere 9 (7), e02311.
Piao, S., Friedlingstein, P., Ciais, P., Viovy, N., Demarty, J., 2007. Growing season extension and its impact on terrestrial carbon cycle in the Northern Hemisphere over the past 2 decades. Global Biogeochemical Cycles 21 (3).
Perkins-Kirkpatrick, S.E., Lewis, S.C., 2020. Increasing trends in regional heatwaves. Nature communications 11 (1), 3357.
Restrepo-Coupe, N., Da Rocha, H.R., Hutyra, L.R., Da Araujo, A.C., Borma, L.S., Christoffersen, B., Cabral, O.M., De Camargo, P.B., Cardoso, F.L., Da Costa, A.C.L., Fitzjarrald, D.R., 2013. What drives the seasonality of photosynthesis across the Amazon basin? A cross-site analysis of eddy flux tower measurements from the Brasil flux network. Agricultural and Forest Meteorology 182, 128–144.
Rotenberg, E., Yakir, D., 2010. Contribution of semi-arid forests to the climate system. Science 327 (5964), 451–454.
Still, C.J., Page, G., Rastogi, B., Griffith, D.M., Aubrecht, D.M., Kim, Y., Burns, S.P., Hanson, C.V., Kwon, H., Hawkins, L., Meinzer, F.C., 2022. No evidence of canopy-scale leaf thermoregulation to cool leaves below air temperature across a range of forest ecosystems. Proceedings of the National Academy of Sciences 119 (38), e2205682119.
Still, C., Powell, R., Aubrecht, D., Kim, Y., Helliker, B., Roberts, D., Richardson, A.D., Goulden, M., 2019. Thermal imaging in plant and ecosystem ecology: applications and challenges. Ecosphere 10 (6), e02768.

Still, C.J., Rastogi, B., Page, G.F., Griffith, D.M., Sibley, A., Schulze, M., Hawkins, L., Pau, S., Detto, M., Helliker, B.R., 2021. Imaging canopy temperature: shedding (thermal) light on ecosystem processes. New Phytologist 230 (5), 1746–1753.
Tiwari, S., Srivastava, A.K., Bisht, D.S., Parmita, P., Srivastava, M.K., Attri, S.D., 2013. Diurnal and seasonal variations of black carbon and PM2. 5 over New Delhi, India: Influence of meteorology. Atmospheric Research 125, 50–62.
Valavi, R., Guillera-Arroita, G., Lahoz-Monfort, J.J., Elith, J., 2022. Predictive performance of presence-only species distribution models: a benchmark study with reproducible code. Ecological Monographs 92 (1), e01486.
Van Zyl, J.J., 2001. The Shuttle Radar Topography Mission (SRTM): a breakthrough in remote sensing of topography. Acta Astronautica 48 (5-12), 559–565.
Vialet-Chabrand, S.I.L.V.È.R.E., Dreyer, E., Brendel, O., 2013. Performance of a new dynamic model for predicting diurnal time courses of stomatal conductance at the leaf level. Plant, cell & environment 36 (8), 1529–1546.
Wang, H., Yan, S., Ciais, P., Wigneron, J.P., Liu, L., Li, Y., Fu, Z., Ma, H., Liang, Z., Wei, F., Wang, Y., 2022. Exploring complex water stress–gross primary production relationships: Impact of climatic drivers, main effects, and interactive effects. Global Change Biology. https://doi.org/10.1111/gcb.16201.
Wright, I.J., Dong, N., Maire, V., Prentice, I.C., Westoby, M., Díaz, S., Gallagher, R.V., Jacobs, B.F., Kooyman, R., Law, E.A., Leishman, M.R., 2017. Global climatic drivers of leaf size. Science 357 (6354), 917–921.
Wu, J., Serbin, S.P., Ely, K.S., Wolfe, B.T., Dickman, L.T., Grossiord, C., Michaletz, S.T., Collins, A.D., Detto, M., McDowell, N.G., Wright, S.J., 2020. The response of stomatal conductance to seasonal drought in tropical forests. Global change biology 26 (2), 823–839.
Wuenscher, J.E., 1970. The effect of leaf hairs of Verbascum thapsus on leaf energy exchange. New Phytologist 69 (1), 65–73.
Yuan, W., Zheng, Y., Piao, S., Ciais, P., Lombardozzi, D., Wang, Y., Ryu, Y., Chen, G., Dong, W., Hu, Z., Jain, A.K., 2019. Increased atmospheric vapor pressure deficit reduces global vegetation growth. Science advances 5 (8), eaax1396.
Zhang, K., Zhu, G., Ma, J., Yang, Y., Shang, S., Gu, C., 2019. Parameter analysis and estimates for the MODIS evapotranspiration algorithm and multiscale verification. Water Resources Research 55 (3), 2211–2231.
Zhang, K., Zhu, G., Ma, N., Chen, H., Shang, S., 2022. Improvement of evapotranspiration simulation in a physically based ecohydrological model for the groundwater–soil–plant–atmosphere continuum. Journal of Hydrology 613, 128440.
Zhang, Y., Xia, C., Zhang, X., Cheng, X., Feng, G., Wang, Y., Gao, Q., 2021. Estimating the maize biomass by crop height and narrowband vegetation indices derived from UAV-based hyperspectral images. Ecological Indicators 129, 107985.